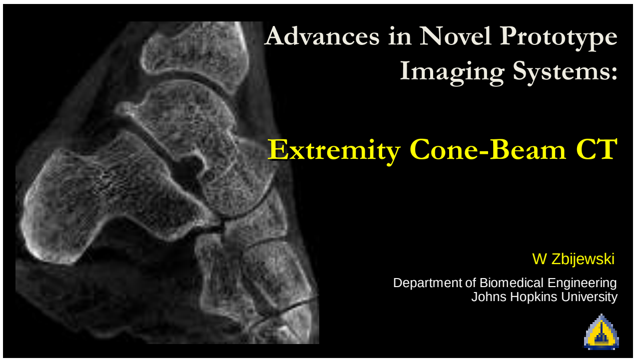
Advances in Novel Prototype
Imaging Systems:
Extremity Cone-Beam CT
W Zbijewski
Department of Biomedical Engineering
Johns Hopkins University


The I-STAR Laboratory
istar.jhu.edu
JH Siewerdsen, JW Stayman, A Sisniega,
M Brehler, Q Cao, S Subramanian
Carestream Health
J Yorkston, W Huang, N Packard, E Wang, D Foos
JHU and JHMI
N Charon, M Mahesh, K. Taguchi, X Cao, J Crane,
C Morris, G Osgood, K Mosley, S Demehri, JA Carrino,
G Thawait, D Shakoor, A. Machado
Funding Support
Carestream Health
NIH R01-EB-018896
NIH R01-EB-025470
NIH R21-AR-062293
NIH R21-CA-208821
US Army NSRDEC W911QY-14-C-0014

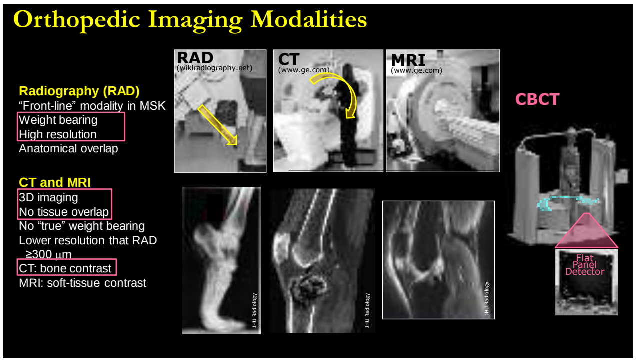
Orthopedic Imaging Modalities
Radiography (RAD)
"Front-line" modality in MSK
Weight bearing
High resolution
Anatomical overlap
CT and MRI
3D imaging
No tissue overlap
No "true" weight bearing
Lower resolution that RAD
≥300 μm
CT: bone contrast
MRI: soft-tissue contrast
RAD
(wikiradiography.net)
CT
(www.ge.com)
MRI
(www.ge.com)
CBCT
Flat
Panel
Detector
JHU Radiology
JHU Radiology
JHU Radiology

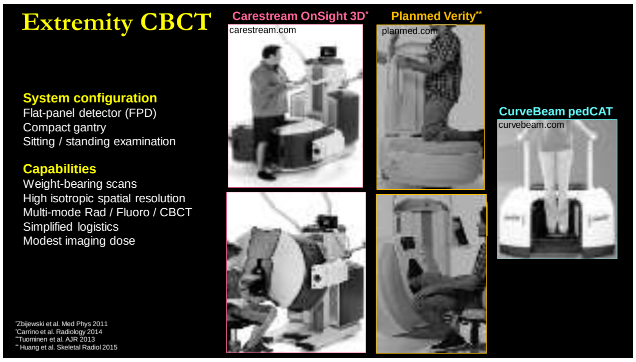
Extremity CBCT
Carestream OnSight 3D*
carestream.com
Planmed Verity**
planmed.com
CurveBeam pedCAT
curvebeam.com
System configuration
Flat-panel detector (FPD)
Compact gantry
Sitting / standing examination
Capabilities
Weight-bearing scans
High isotropic spatial resolution
Multi-mode Rad / Fluoro / CBCT
Simplified logistics
Modest imaging dose
*Zbijewski et al. Med Phys 2011
*Carrino et al. Radiology 2014
**Tuominen et al. AJR 2013
** Huang et al. Skeletal Radiol 2015

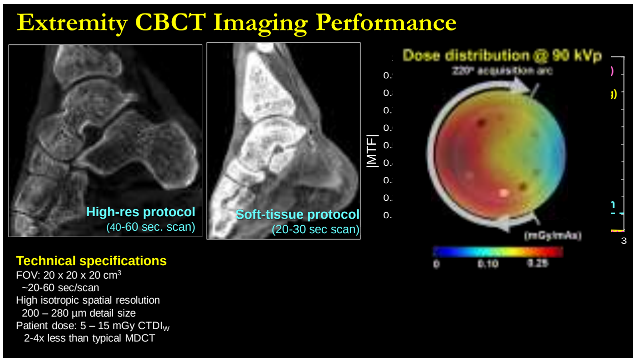
Extremity CBCT Imaging Performance
High-res protocol
(40-60 sec. scan)
Soft-tissue protocol
(20-30 sec scan)
Dose distribution @ 90 kVp
|MTF|
(mGy/mAs)
0
0.10
0.25
Technical specifications
FOV: 20 x 20 x 20 cm3
~20-60 sec/scan
High isotropic spatial resolution
200 – 280 µm detail size
Patient dose: 5 – 15 mGy CTDIW
2-4x less than typical MDCT

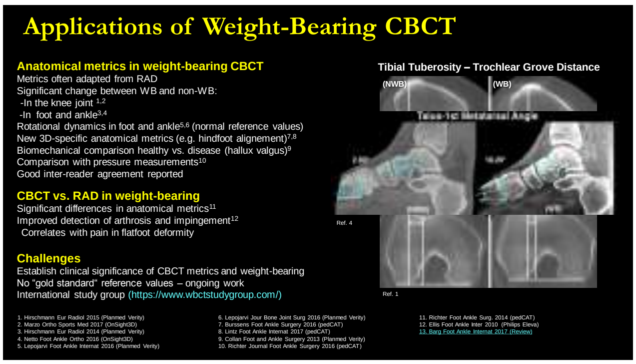
Applications of Weight-Bearing CBCT
Anatomical metrics in weight-bearing CBCT
Metrics often adapted from RAD
Significant change between WB and non-WB:
-In the knee joint 1,2
-In foot and ankle3,4
Rotational dynamics in foot and ankle5,6 (normal reference values)
New 3D-specific anatomical metrics (e.g. hindfoot alignement)7,8
Biomechanical comparison healthy vs. disease (hallux valgus)9
Comparison with pressure measurements10
Good inter-reader agreement reported
CBCT vs. RAD in weight-bearing
Significant differences in anatomical metrics11
Improved detection of arthrosis and impingement12
Correlates with pain in flatfoot deformity
Challenges
Establish clinical significance of CBCT metrics and weight-bearing
No "gold standard" reference values – ongoing work
International study group (https://www.wbctstudygroup.com/)
Tibial Tuberosity – Trochlear Grove Distance
(NWB)
(WB)
Ref. 4
Ref. 1
1. Hirschmann Eur Radiol 2015 (Planmed Verity)
2. Marzo Ortho Sports Med 2017 (OnSight3D)
3. Hirschmann Eur Radiol 2014 (Planmed Verity)
4. Netto Foot Ankle Ortho 2016 (OnSight3D)
5. Lepojarvi Foot Ankle Internat 2016 (Planmed Verity)
6. Lepojarvi Jour Bone Joint Surg 2016 (Planmed Verity)
7. Burssens Foot Ankle Surgery 2016 (pedCAT)
8. Lintz Foot Ankle Internat 2017 (pedCAT)
9. Collan Foot and Ankle Surgery 2013 (Planmed Verity)
10. Richter Journal Foot Ankle Surgery 2016 (pedCAT)
11. Richter Foot Ankle Surg. 2014 (pedCAT)
12. Ellis Foot Ankle Inter 2010 (Philips Eleva)
13. Barg Foot Ankle Internat 2017 (Review)

Joint Space Analysis in OA

JSW ME

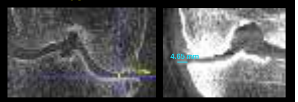

Joint Space Width (JSW)
Detection and staging of OA
Currently measured with weight-bearing RAD
More accurate positioning with CBCT[1]
Improved sensitivity
High inter-reader agreement
Weight-bearing (WB) vs. Non-weight bearing (NWB)[1]
Significant difference in JSW for OA
No significant difference in JSW for non-OA

Additional metrics accessible to CBCT
Meniscal extrusion (ME)
Weight bearing aids detection of ME[2]
ME changes between WB and non-WB in OA patients[1]
Osteophytes and cysts in OA
Higher sensitivity and specificity in CBCT than RAD[2]

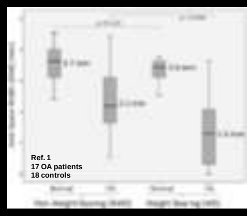

1. Thawait Eur Radiol 2015 (OnSight3D)
2. Segal Phys Sportsmed 2015 (pedCAT modified for knees)

Quantitative Imaging of Bone Health

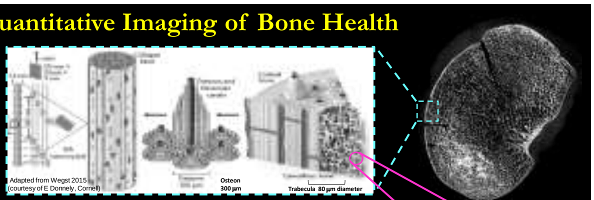

Bone microstructure and remodeling
Bone responds to load distribution
Continuous remodeling affects microstructure and composition

Clinical applications
Risk of fracture
Osteoporosis, bone loss
Fracture healing
Early osteoarthritis
Changes in bone may precede cartilage loss
Implant biomechanics


Adapted from van der Linden and Weinans 2007

Quantitative Imaging of Bone Health

Bone microstructure
80 – 150 um feature size
Trabecular Thickness (Tb.Th), Spacing (Tb.Sp)…
Bone Volume
Cortical thickness, porosity…
Limited to pre-clinical Micro-CT (µCT)
…or HR-pQCT

Bone composition
Requires high HU uniformity and reproducibility
Bone Mineral Density (BMD)
X-ray imaging
DEXA / qCT
Bone Marrow Edema (BME)
Increased fluid content
T2-weighted MRI

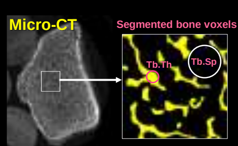

Extremity CBCT with CMOS Detectors

CMOS Detector
Crystalline Silicon
- Fast read-out: 30 fr/sec for 30x30 cm
- Limited wafer size - tiling

Active pixels
- Low electronic noise: ~100 electrons / pixel

High fill factor
- Improved spatial resolution: ≤100 μm pixels

aSi Flat Panel Detector (FPD)
Mainstay of CBCT
Amorphous Silicon (aSi)
- 7.5 fr/sec for 30x30 cm

Passive pixels
- ~1500 electrons/pixel dark noise
- ≥100 μm pixel pitch

	a-Si:H FPD-CBCT	CMOS-CBCT
Detector	Varian PaxScan2530	Dalsa Xineos3030
Pixel size	139 μm	99 μm
e^- noise	~2000 e^-	~140 e^-
Frame Rate	7.5 fps	30 fps

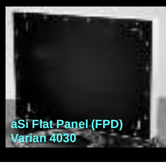

System Optimization Framework

Design Tradeoffs
Resolution / Scintillator Thickness / Magnification
X-ray source power / Focal Spot / Beam Energy
Compact geometry / Scatter
Soft-tissue visualization / Noise
Dose

Modeling of imaging performance

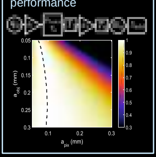

Benchtop experiments

Clinical prototype
-delivered March 2017
-clinical pilot study 2018

Cao SPIE 2017, SPIE 2018, Med Phys 2017

System Modeling: Cascaded Systems Analysis

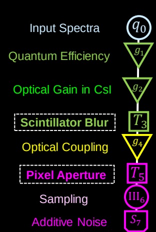

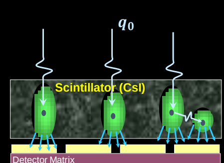

$$MTF = T_3 T_{Ktot} T_5$$

$$NPS = \overline{q_0} a_{pd}^4 \overline{g_1 g_2 g_4}(1 + \overline{g_4} P_K T_3^2) T_5^2 ** III_6 + S_7$$

Siewerdsen et al. Med Phys 1997
Rabbani et al. JOSA 1987

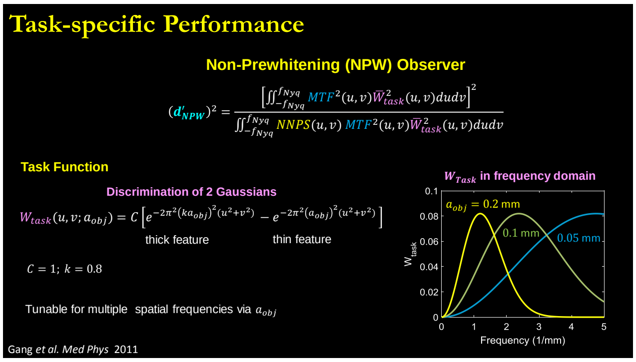
Task-specific Performance
Non-Prewhitening (NPW) Observer
$$(d'_{NPW})^2 = \frac{\left[\iint_{-f_{Nyq}}^{f_{Nyq}} MTF^2(u,v)\overline{W}^2_{task}(u,v)dudv\right]^2}{\iint_{-f_{Nyq}}^{f_{Nyq}} NNPS(u,v)\ MTF^2(u,v)\overline{W}^2_{task}(u,v)dudv}$$
Task Function
Discrimination of 2 Gaussians
$$W_{task}(u,v;a_{obj}) = C\left[e^{-2\pi^2(ka_{obj})^2(u^2+v^2)} - e^{-2\pi^2(a_{obj})^2(u^2+v^2)}\right]$$
thick feature
thin feature
$C = 1;\ k = 0.8$
Tunable for multiple spatial frequencies via a_{obj}
W_{Task} in frequency domain
a_{obj} = 0.2 mm
0.1 mm
0.05 mm
W_{task}
Frequency (1/mm)
Gang *et al. Med Phys* 2011

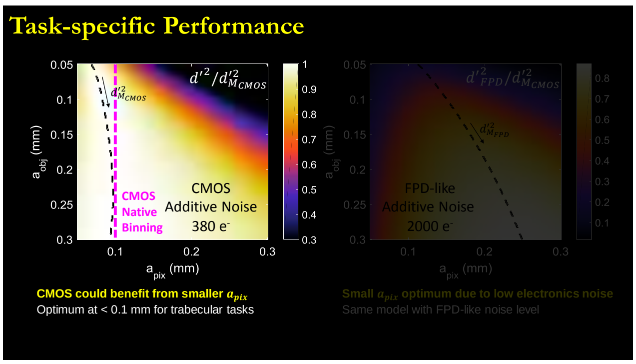
Task-specific Performance
$d'^2/d'^2_{M_{CMOS}}$
$d'^2_{M_{CMOS}}$
CMOS Native Binning
CMOS Additive Noise 380 e⁻
a_{obj} (mm)
a_{pix} (mm)
$d'^2_{FPD}/d'^2_{M_{CMOS}}$
$d'^2_{M_{FPD}}$
FPD-like Additive Noise 2000 e⁻
CMOS could benefit from smaller a_{pix}
Optimum at < 0.1 mm for trabecular tasks
Small a_{pix} optimum due to low electronics noise
Same model with FPD-like noise level

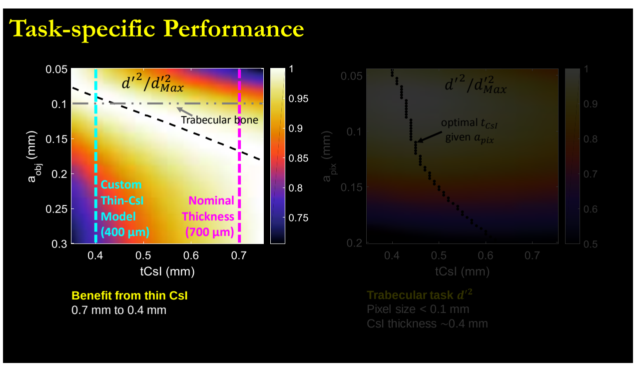
Task-specific Performance
d'^2/d'^2_{Max}
Trabecular bone
Custom Thin-CsI Model (400 μm)
Nominal Thickness (700 μm)
a_{obj} (mm)
tCsI (mm)
optimal t_{CsI} given a_{pix}
a_{pix} (mm)
Benefit from thin CsI
0.7 mm to 0.4 mm
Trabecular task d'^2
Pixel size < 0.1 mm
CsI thickness ~0.4 mm

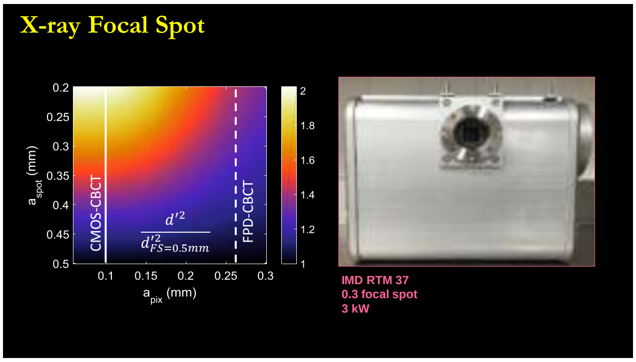
X-ray Focal Spot
a_{spot} (mm)
0.2
0.25
0.3
0.35
0.4
0.45
0.5
0.1
0.15
0.2
0.25
0.3
a_{pix} (mm)
CMOS-CBCT
FPD-CBCT
$\frac{d'^2}{d'^2_{FS=0.5mm}}$
2
1.8
1.6
1.4
1.2
1
IMD RTM 37
0.3 focal spot
3 kW

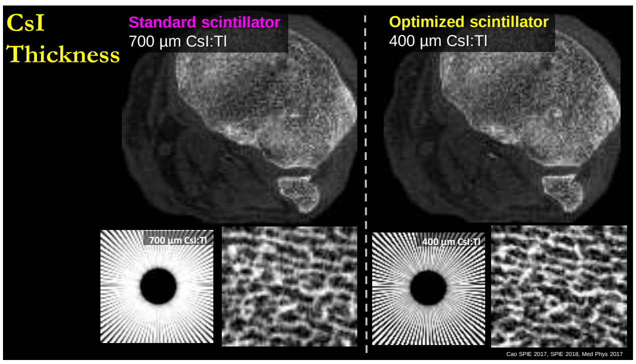
CsI Thickness
Standard scintillator
700 µm CsI:Tl
Optimized scintillator
400 µm CsI:Tl
700 µm CsI:Tl
400 µm CsI:Tl
Cao SPIE 2017, SPIE 2018, Med Phys 2017

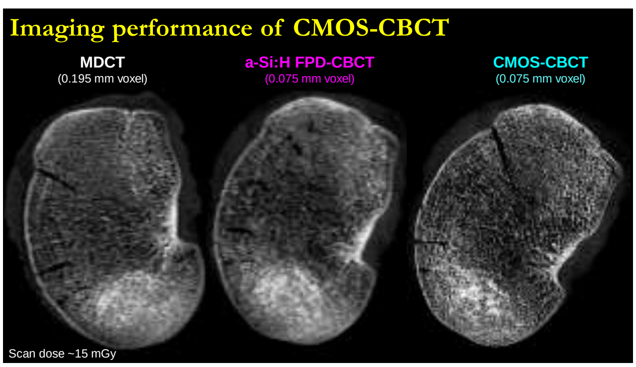
Imaging performance of CMOS-CBCT
MDCT
(0.195 mm voxel)
a-Si:H FPD-CBCT
(0.075 mm voxel)
CMOS-CBCT
(0.075 mm voxel)
Scan dose ~15 mGy

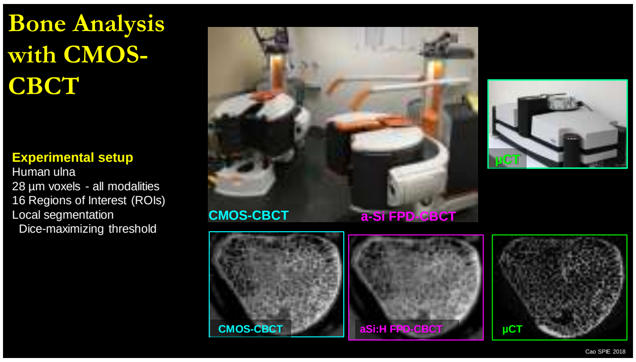
Bone Analysis with CMOS-CBCT
Experimental setup
Human ulna
28 µm voxels - all modalities
16 Regions of Interest (ROIs)
Local segmentation
Dice-maximizing threshold
µCT
CMOS-CBCT
a-Si FPD-CBCT
CMOS-CBCT
aSi:H FPD-CBCT
µCT
Cao SPIE 2018

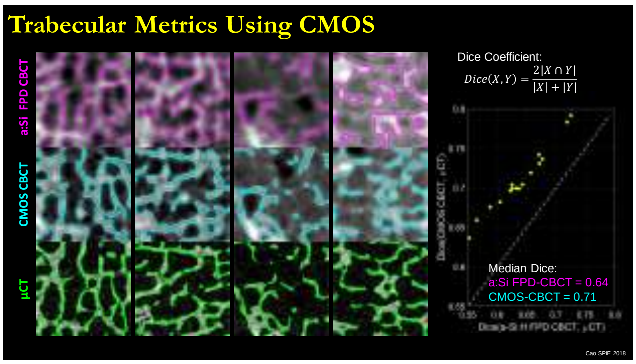
Trabecular Metrics Using CMOS
a:Si FPD CBCT
CMOS CBCT
µCT
Dice Coefficient:
$Dice(X,Y) = \frac{2|X \cap Y|}{|X| + |Y|}$
Median Dice:
a:Si FPD-CBCT = 0.64
CMOS-CBCT = 0.71
Cao SPIE 2018

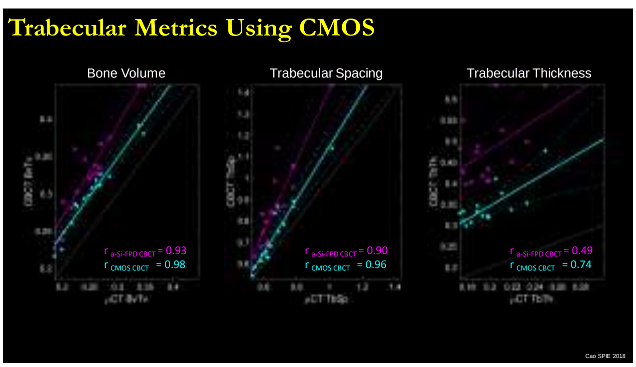
Trabecular Metrics Using CMOS
Bone Volume
Trabecular Spacing
Trabecular Thickness
$r_{a\text{-}Si\text{-}FPD\ CBCT} = 0.93$
$r_{CMOS\ CBCT} = 0.98$
$r_{a\text{-}Si\text{-}FPD\ CBCT} = 0.90$
$r_{CMOS\ CBCT} = 0.96$
$r_{a\text{-}Si\text{-}FPD\ CBCT} = 0.49$
$r_{CMOS\ CBCT} = 0.74$
Cao SPIE 2018

Artifacts and Corrections: Motion

Motion contaminated

Au
T = R
$\hat{T} = \epsilon$

n
ess

Motior
Dimensi
esentation:
$T(\theta,$
ots

Regul
Smoothr
ROI (p_k)
$R($
$k=1$ $\theta=2$

Autofocus motion compensation
Find motion using image sharpness criterion
No fiducials, no prior images
Applicable to local ROIs
CMA-ES optimization

A. Sisniega Phys Med Biol 2017

Artifacts and Corrections: Motion

Benchtop experiment
1 mm step motion

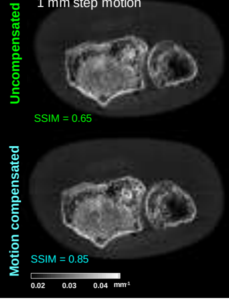

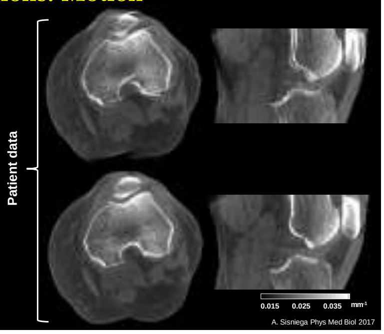

A. Sisniega Phys Med Biol 2017

Quantitative Imaging of Bone Health

Bone microstructure
80 – 150 um feature size
Cortical thickness, porosity…
Bone Volume
Trabecular Thickness (Tb.Th), Spacing (Tb.Sp)…
Limited to pre-clinical Micro-CT (μCT)
…or HR-pQCT

Bone composition
Requires high HU uniformity and reproducibility
Bone Mineral Density (BMD)
X-ray imaging
DEXA / qCT
Bone Marrow Edema (BME)
Increased fluid content
T2-weighted MRI

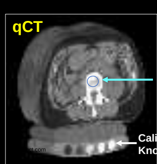

Quantitative Accuracy in CBCT Using MBIR

Polyenergetic Model-Based Reconstruction (MBIR)
Measurement model assuming K-base materials:

$$t_i = \int I_i(E)\exp\left(\sum_k^K -m_k(E)\, s_{ik}(\rho)\right) dE$$

Estimate voxel composition from density:[1]

$$s_{ik}(\rho) = \sum_j^P a_{ij}\rho_j f_k(\rho_j)$$

Use ideal mixture model to establish f_k
Calibrated to Gammex Dual Energy Inserts

Scatter Correction
"Sparse Monte Carlo"
Low-number of photons, projection subsampling + kernel denoising[2]

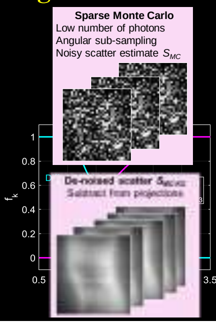

1. Elbakri 2001
2. Siniega 2015

BMD Reproducibility and Accuracy

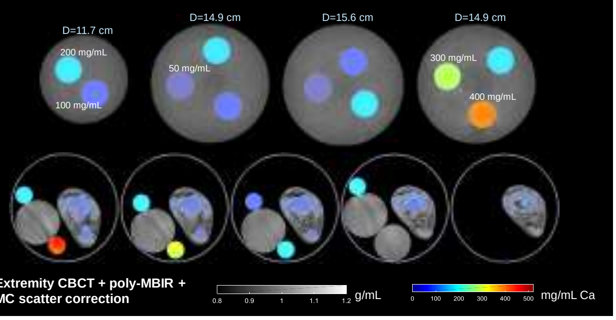

Extremity CBCT + poly-MBIR + MC scatter correction

BMD Reproducibility and Accuracy

Variability across imaging configurations

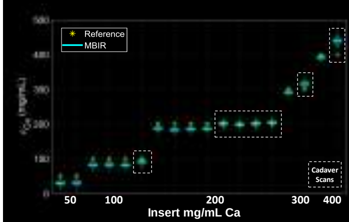

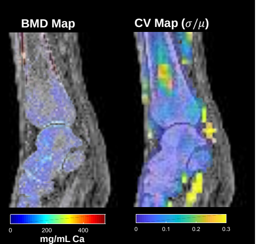

Summary

Extremities CBCT
3D weight-bearing imaging
Isotropic spatial resolution (~250 μm)
Improved resolution using optimized CMOS (~150 μm)

Quantitative bone imaging
In-vivo evaluation of bone microarchitecture
BMD measurements
MBIR + artifact correction

New directions
Dual-energy assessment of bone composition
Finite element models (FEM)
Shape models and joint space mapping
New scintillators
Model-based reconstruction in presence of metal
High-resolution MDCT
~250 μm detail size
Texture analysis